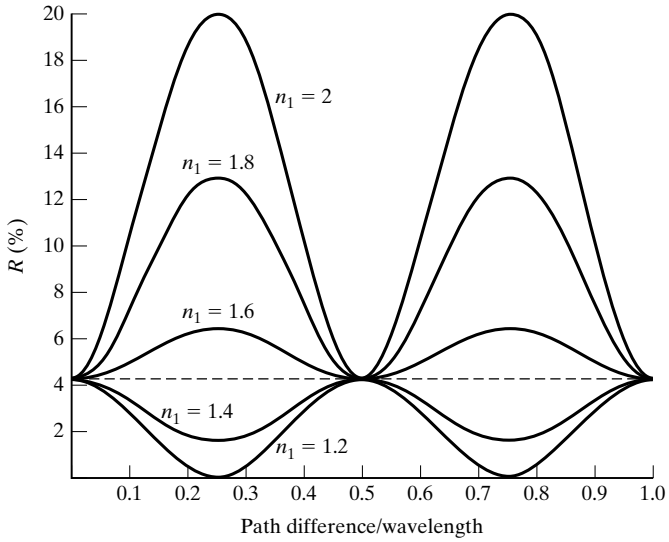

22 Theory of Multilayer Films

INTRODUCTION

The physics of interference in single-layer dielectric films, in its essentials, should already be familior to you. Many useful and interesting applications of thin films, however, make use of multilayer stacks of films. It is possible to evaporate multiple layers while maintaining control over both refractive index (choice of material) and individual layer thickness. Such techniques provide a great deal of flexibility in designing interference coatings with almost any specified frequency-dependent reflectance or transmittance characteristics. Useful applications of such coatings include antireflecting multilayers for use on the lenses of optical instruments and display windows; multipurpose broad and narrow band-pass filters, available from near ultraviolet to near infrared wavelengths; thermal reflectors and cold mirrors, which reflect and transmit infrared, respectively, and are used in projectors; dichroic mirrors consisting of band-pass filters deposited on the faces of prismatic beam splitters to divide light into red, green, and blue channels in color television cameras; and highly reflecting dielectric mirrors for use in gas lasers and in Fabry-Perot interferometers.

Computer techniques have made routine the rather detailed calculations involved in the analysis of multilayer film performance. The design of a multilayer stack that will meet arbitrary prespecified characteristics, however, remains a formidable task. In this chapter we develop a *transfer matrix* to represent the film and characterize its performance. The approach differs from that used in treating multiple reflections from a thin film. There we added the amplitudes of all the individual reflected or transmitted beams to find the resultant reflectance or transmittance. It will be more efficient, in the general treatment that follows, to consider all transmitted or reflected beams as already summed in corresponding electric fields that satisfy the general boundary conditions required by Maxwell's equations.

The relationships we require from electromagnetic theory are summarized here. The energy of a plane, electromagnetic wave propagates in the direction of the Poynting vector, given by

$$\vec{\mathbf{S}} = \varepsilon_0 c^2 \vec{\mathbf{E}} \times \vec{\mathbf{B}} \tag{1}$$

The magnitudes of electric and magnetic fields in the wave are related by

$$E = vB \tag{2}$$

where the wave speed is related to the the refractive index n by

$$n = \frac{c}{v} \tag{3}$$

The wave speed in vacuum is a constant, equal to

$$c = \frac{1}{\sqrt{\varepsilon_0 \mu_0}} \tag{4}$$

where ε_0 and μ_0 are the permittivity and permeability, respectively, of free space. Combining Eqs. (2), (3), and (4), the magnitudes of the magnetic and electric fields can also be related by

$$B = \frac{E}{v} = \left(\frac{n}{c}\right) E = n\sqrt{\varepsilon_0 \mu_0} E \tag{5}$$

1 TRANSFER MATRIX

Our analysis is carried out in terms of the quantities defined in Figure 1. An incident beam is shown, with $\vec{\mathbf{E}}$ chosen for the moment in a direction perpendicular to the plane of incidence. (Keep in mind, however, that at normal incidence $E_\perp$ and $E_\parallel$ are equivalent since a unique plane of incidence cannot be specified.) The beam undergoes external reflection at the plane interface (a) separating the external medium of index n_0 from the nonmagnetic ($\mu = \mu_0$) film of index n_1. The transmitted portion of the beam undergoes an internal

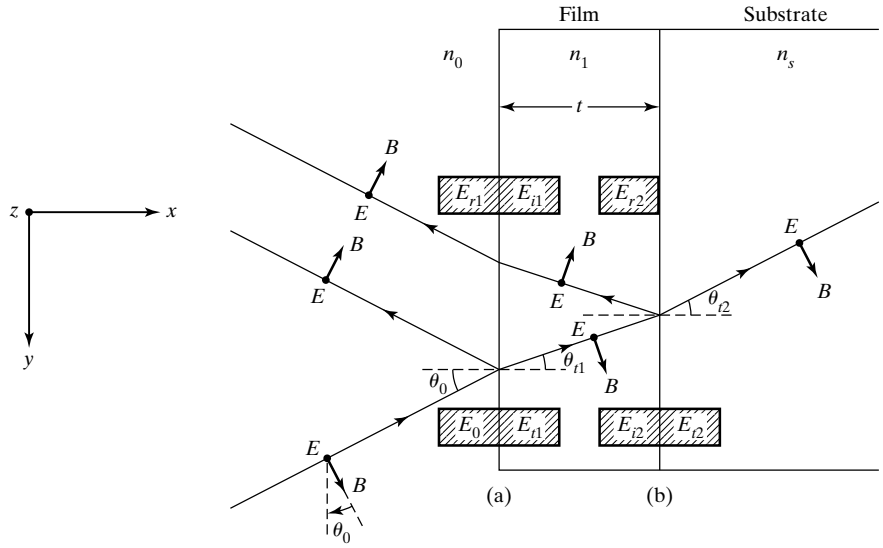

Figure 1 Reflection of a beam from a single layer. The diagram defines quantities used in applying boundary conditions to write Eqs. (6)–(9). Note that a bold dot is used to denote directions perpendicular to the plane of incidence.

reflection and transmission at the plane interface (b) separating the film from the substrate of index n_s. Along each beam the $\vec{\mathbf{E}}$-field is shown—by the usual dot notation—to be pointing out of the page ($-z$-direction), and the $\vec{\mathbf{B}}$-field is shown in a direction consistent with Eq. (1). Notice that the y-component of $\vec{\mathbf{B}}$ must reverse on reflection. The insets define a terminology for the magnitudes of the electric fields *at the boundaries* (a) and (b). For example, E_{r1} represents the sum of all the multiply reflected beams at interface (a) in the process of emerging from the film, E_{i2} represents the sum of all the multiple beams incident at interface (b) and directed toward the substrate, and so on. In this way, we account for multiple beams in the interference.

We assume that the film is both homogeneous and isotropic. We assume further that the film thickness is of the order of the wavelength of light, so that the path difference between multiply reflected and transmitted beams remains small compared with the coherence length of the monochromatic light. This ensures that the beams are essentially coherent. The width of the incident beam, finally, is assumed to be large compared with its lateral displacement due to the many reflections that contribute significantly to the resultant reflected and transmitted beams.

Boundary conditions for the electric and magnetic fields of plane waves incident on the interfaces (a) and (b) follow from Maxwell's equations and are simply stated: The tangential components of the resultant $\vec{\mathbf{E}}$- and $\vec{\mathbf{B}}$-fields are continuous across the interface: that is, their magnitudes on either side are equal. For the case considered in Figure 1, $\vec{\mathbf{E}}$ is everywhere tangent to the planes at (a) and (b), whereas $\vec{\mathbf{B}}$ consists of both a tangential component (y-direction) and a perpendicular component (x-direction). Thus the boundary conditions for the electric field at the two interfaces become

$$E_a = E_0 + E_{r1} = E_{t1} + E_{i1} \tag{6}$$

$$E_b = E_{i2} + E_{r2} = E_{t2} \tag{7}$$

Corresponding equations for the magnetic field are

$$B_a = B_0 \cos\theta_0 - B_{r1} \cos\theta_0 = B_{t1} \cos\theta_{t1} - B_{i1} \cos\theta_{t1} \tag{8}$$

$$B_b = B_{i2} \cos\theta_{t1} - B_{r2} \cos\theta_{t1} = B_{t2} \cos\theta_{t2} \tag{9}$$

Rewriting Eqs. (8) and (9) in terms of electric fields with the help of Eq. (5),

$$B_a = \gamma_0(E_0 - E_{r1}) = \gamma_1(E_{t1} - E_{i1}) \tag{10}$$

$$B_b = \gamma_1(E_{i2} - E_{r2}) = \gamma_s E_{t2} \tag{11}$$

where we have written

$$\gamma_0 \equiv n_0\sqrt{\varepsilon_0\mu_0}\cos\theta_0 \tag{12}$$

$$\gamma_1 \equiv n_1\sqrt{\varepsilon_0\mu_0}\cos\theta_{t1} \tag{13}$$

$$\gamma_s \equiv n_s\sqrt{\varepsilon_0\mu_0}\cos\theta_{t2} \tag{14}$$

Now E_{i2} differs from E_{t1} only because of a phase difference δ that develops due to one traversal of the film. The optical path length Δ associated with *two* traversals of the thin film is $\Delta = 2n_1 t\cos(\theta_{t1})$. Thus the optical path length Δ_1

associated with *one* traversal is $\Delta_1 = \Delta/2 = n_1 t \cos(\theta_{t1})$, and phase difference δ that develops due to one traversal of the film is

$$\delta = k_0 \Delta_1 = \left(\frac{2\pi}{\lambda_0}\right) n_1 t \cos \theta_{t1} \tag{15}$$

Thus,

$$E_{i2} = E_{t1} e^{-i\delta} \tag{16}$$

In the same way,

$$E_{i1} = E_{r2} e^{-i\delta} \tag{17}$$

Using Eqs. (16) and (17), we may eliminate the fields E_{i2} and E_{r2} in the boundary conditions at (b), expressed by Eqs. (7) and (11), as follows:

$$E_b = E_{t1} e^{-i\delta} + E_{i1} e^{i\delta} = E_{t2} \tag{18}$$

$$B_b = \gamma_1 (E_{t1} e^{-i\delta} - E_{i1} e^{i\delta}) = \gamma_s E_{t2} \tag{19}$$

Disregarding for the moment the rightmost members, these equations may be solved simultaneously for E_{t1} and E_{i1} in terms of E_b and B_b, yielding

$$E_{t1} = \left(\frac{\gamma_1 E_b + B_b}{2\gamma_1}\right) e^{i\delta} \tag{20}$$

$$E_{i1} = \left(\frac{\gamma_1 E_b - B_b}{2\gamma_1}\right) e^{-i\delta} \tag{21}$$

Finally, substituting the expressions from Eqs. (20) and (21) into the Eqs. (6) and (10) for boundary (a), the result is

$$E_a = E_b \cos \delta + B_b \left(\frac{i \sin \delta}{\gamma_1}\right) \tag{22}$$

$$B_a = E_b (i\gamma_1 \sin \delta) + B_b \cos \delta \tag{23}$$

where we have used the Euler identities

$$2 \cos \delta \equiv e^{i\delta} + e^{-i\delta} \quad \text{and} \quad 2i \sin \delta \equiv e^{i\delta} - e^{-i\delta}$$

Equations (22) and (23) relate the net fields at one boundary with those at the other. They may be written in matrix form as

$$\begin{bmatrix} E_a \\ B_a \end{bmatrix} = \begin{bmatrix} \cos \delta & \dfrac{i \sin \delta}{\gamma_1} \\ i\gamma_1 \sin \delta & \cos \delta \end{bmatrix} \begin{bmatrix} E_b \\ B_b \end{bmatrix} \tag{24}$$

The 2×2 matrix is called the *transfer matrix* of the film, represented in general by

$$M = \begin{bmatrix} m_{11} & m_{12} \\ m_{21} & m_{22} \end{bmatrix} \tag{25}$$

If boundary (b) is the interface of another film layer, rather than the substrate, Eq. (24) is still valid. The fields E_b and B_b are then related to the fields E_c and B_c at the back boundary of the second film layer by a second transfer matrix. Generalizing, then for a multilayer of arbitrary number N of layers,

$$\begin{bmatrix} E_a \\ B_a \end{bmatrix} = M_1 M_2 M_3 \cdots M_N \begin{bmatrix} E_N \\ B_N \end{bmatrix}$$

An overall transfer matrix, M_T, representing the entire multilayer stack is the product of the individual transfer matrices, in the order in which the light encounters them,

$$M_T = M_1 M_2 M_3 \cdots M_N \tag{26}$$

We return now to Eqs. (6), (7), (10), and (11) to make use of those members previously ignored in first finding the transfer matrix. Those remaining equations are

$$E_a = E_0 + E_{r1} \tag{27}$$

$$E_b = E_{t2} \tag{28}$$

$$B_a = \gamma_0 (E_0 - E_{r1}) \tag{29}$$

$$B_b = \gamma_s E_{t2} \tag{30}$$

For the fields represented by Eqs. (27) to (30), Eq. (24) takes the form,

$$\begin{bmatrix} E_0 + E_{r1} \\ \\ \gamma_0 (E_0 - E_{r1}) \end{bmatrix} = \begin{bmatrix} \cos\delta & \dfrac{i \sin\delta}{\gamma_1} \\ \\ i\gamma_1 \sin\delta & \cos\delta \end{bmatrix} \begin{bmatrix} E_{t2} \\ \\ \gamma_s E_{t2} \end{bmatrix} = \begin{bmatrix} m_{11} & m_{12} \\ m_{21} & m_{22} \end{bmatrix} \begin{bmatrix} E_{t2} \\ \gamma_s E_{t2} \end{bmatrix} \tag{31}$$

where in the last equality we have used the generic form of the transfer matrix given in Eq. (25). The last equality in Eq. (31) defines the transfer matrix elements, m_{11}, m_{12}, m_{21}, and m_{22} for the case at hand.

Equation (31) is equivalent to the two equations,

$$E_0 + E_{r1} = m_{11} E_{t2} + m_{12} \gamma_s E_{t2}$$

$$\gamma_0 (E_0 - E_{r1}) = m_{21} E_{t2} + m_{22} \gamma_s E_{t2}$$

Dividing through these two equations by E_0 and making use of the reflection coefficient r and transmission coefficient t, defined as

$$r \equiv \frac{E_{r1}}{E_0} \quad \text{and} \quad t \equiv \frac{E_{t2}}{E_0} \tag{32}$$

we obtain

$$1 + r = m_{11} t + m_{12} \gamma_s t \tag{33}$$

$$\gamma_0 (1 - r) = m_{21} t + m_{22} \gamma_s t \tag{34}$$

Equations (33) and (34) can be solved for the transmission and reflection coefficients in terms of the transfer-matrix elements to give

$$t = \frac{2\gamma_0}{\gamma_0 m_{11} + \gamma_0\gamma_s m_{12} + m_{21} + \gamma_s m_{22}} \tag{35}$$

$$r = \frac{\gamma_0 m_{11} + \gamma_0\gamma_s m_{12} - m_{21} - \gamma_s m_{22}}{\gamma_0 m_{11} + \gamma_0\gamma_s m_{12} + m_{21} + \gamma_s m_{22}} \tag{36}$$

Equations (35) and (36), together with the transfer-matrix elements, defined by Eqs. (24) and (31), now enable one to evaluate the reflective and transmissive properties of a single or multilayer film represented by the transfer matrix.

Before continuing with applications of these equations, we must take into account the necessary modification of the theory that results when the incident electric field of Figure 1 has the other polarization, that is, in the plane of incidence. Suppose that $\vec{\mathbf{E}}$ is chosen in the original direction of $\vec{\mathbf{B}}$ and $\vec{\mathbf{B}}$ is rotated accordingly to maintain the same wave direction. If the equations are developed along the same lines, one finds that only a minor alteration of the transfer matrix becomes necessary: In the expression for γ_1, Eq. (13), the cosine factor now appears in the denominator rather than in the numerator. Summarizing,

$$\begin{aligned} &\vec{\mathbf{E}} \perp \text{ plane of incidence:} \quad \gamma_1 = n_1\sqrt{\varepsilon_0\mu_0}\cos\theta_{t1} \\ &\vec{\mathbf{E}} \parallel \text{ plane of incidence:} \quad \gamma_1 = n_1\frac{\sqrt{\varepsilon_0\mu_0}}{\cos\theta_{t1}} \end{aligned} \tag{37}$$

Notice that for normal incidence, where $\vec{\mathbf{E}}_\perp$ and $\vec{\mathbf{E}}_\parallel$ are indistinguishable, we have $\cos\theta_{t1} = 1$, and the expressions are equivalent. For oblique incidence, however, results must be calculated for each polarization. An average can be taken for unpolarized light. For example, the reflectance becomes

$$R = \tfrac{1}{2}(R_\parallel + R_\perp) \tag{38}$$

2 REFLECTANCE AT NORMAL INCIDENCE

We apply the theory now for normally incident light, the case most commonly found in practice. Results apply quite well also to cases of near-normal incidence. The beam remains normal at all interfaces, so that all angles of incidence, reflection, and refraction are zero. In Eqs. (12) to (14), the cosine factors in the γ-terms are all unity. The matrix elements from Eq. (24), appropriately modified to become

$$\begin{aligned} m_{11} &= \cos\delta \qquad m_{12} = \frac{i\sin\delta}{n_1\sqrt{\varepsilon_0\mu_0}} \\ m_{21} &= in_1\sqrt{\varepsilon_0\mu_0}\sin\delta \qquad m_{22} = \cos\delta \end{aligned} \tag{39}$$

are substituted into Eq. (36). After cancellation of the constant $\sqrt{\varepsilon_0\mu_0}$ and some simplification, we find

$$r = \frac{n_1(n_0 - n_s)\cos\delta + i(n_0 n_s - n_1^2)\sin\delta}{n_1(n_0 + n_s)\cos\delta + i(n_0 n_s + n_1^2)\sin\delta} \tag{40}$$

The reflectance R, which determines the reflected irradiance, is defined by

$$R = |r|^2 \tag{41}$$

To calculate R, first notice that the reflection coefficient r is complex and that it has the general form

$$r = \frac{A + iB}{C + iD}$$

so that

$$|r|^2 = rr^* = \left(\frac{A + iB}{C + iD}\right)\left(\frac{A - iB}{C - iD}\right) = \frac{A^2 + B^2}{C^2 + D^2}$$

By inspection then, we may write

$$\text{normal incidence} \qquad R = \frac{n_1^2(n_0 - n_s)^2\cos^2\delta + (n_0 n_s - n_1^2)^2\sin^2\delta}{n_1^2(n_0 + n_s)^2\cos^2\delta + (n_0 n_s + n_1^2)^2\sin^2\delta} \tag{42}$$

Example 1

A 400-Å-thick film of ZrO_2 ($n = 2.10$) is deposited on glass ($n = 1.50$). Determine the normal reflectance for sodium light of wavelength $\lambda_0 = 589.3$ nm.

Solution

The phase difference is given by

$$\delta = \frac{2\pi}{\lambda_0}(n_1 t) = \frac{2\pi}{589.3}(2.1)(40) = 0.8956 \text{ rad}$$

so that $\cos\delta = 0.6250$ and $\sin\delta = 0.7806$. Then, substituting into Eq. (42),

$$R = \frac{2.1^2(1 - 1.5)^2(0.6250)^2 + [(1)(1.5) - 2.1^2]^2(0.7806)^2}{2.1^2(1 + 1.5)^2(0.6250)^2 + [(1)(1.5) + 2.1^2]^2(0.7806)^2} = 0.174$$

That is, the irradiance of the reflected beam is 17.4% of the irradiance of the incident beam.

A plot of reflectance versus the optical path difference $\Delta_1 = n_1 t$ associated with one traversal of the film is shown in Figure 2, where the abscissa is calibrated in ratios of Δ_1/λ, with $\lambda = \lambda_0/n_1$ being the wavelength in the film. Each curve corresponds to a different film index, but the glass substrate index has been chosen $n_s = 1.52$ in all cases. The magnitude of the film index n_1 evidently determines whether the reflectance is enhanced (for $n_1 > n_s$) or reduced (for $n_1 < n_s$) from that for uncoated glass. The curves show that quarter-wave thicknesses, or odd multiples thereof, lead either to optimum enhancement (high-reflectance coating) or to maximum reduction (antireflection coating). These minima or maxima points in R can be made to occur at various wavelengths by changing Δ_1 through selection of the film thickness. Notice that for $\Delta_1 = \lambda/2$ or any even multiple of a quarter-wavelength, the reflectance is just that from the uncoated glass. An antireflecting single coat, with $n_1 < n_s$, never reflects more than the uncoated glass at any wavelength. The periodic variation in R with Δ_1, which is proportional to the film thickness, provides a practical way of monitoring film thickness in the course of a film deposition.

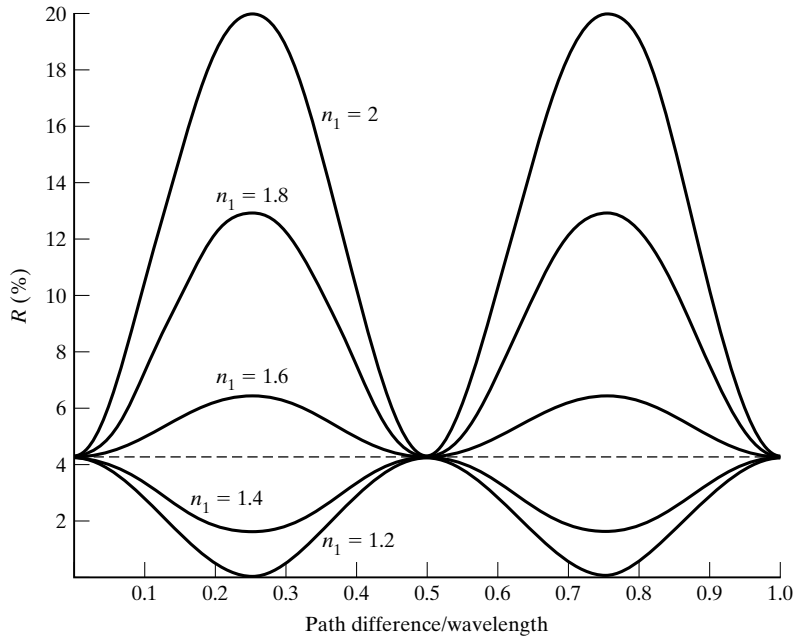

Figure 2 Reflectance from a single film layer of index of refraction n_1 versus normalized path difference. The dashed line represents the uncoated glass substrate of index $n_s = 1.52$.

The important case of quarter-wave film thickness,

$$t = \frac{\lambda}{4} = \frac{\lambda_0}{4n_1}$$

makes the phase difference, Eq. (15), $\delta = 2\pi n_1 t/\lambda_0 = \pi/2$, so that $\cos\delta = 0$ and $\sin\delta = 1$. In this case, Eq. (42) reduces to

$$\text{normal incidence quarter-wave thickness} \quad R = \left(\frac{n_0 n_s - n_1^2}{n_0 n_s + n_1^2}\right)^2 \tag{43}$$

From Eq. (43), it follows that a perfectly *antireflecting* film can be fabricated with a coating of $\lambda/4$ thickness and refractive index $n_1 = \sqrt{n_0 n_s}$. If the substrate is glass, with $n_s = 1.52$, the ideal index for a nonreflecting coating is $n_1 = 1.23$, assuming an ambient with $n_0 = 1$. A compromise choice among available coating materials is a film of MgF_2, with $n_1 = 1.38$. For this film, Eq. (43) predicts a reflectance of 1.3% in the visible region, where the uncoated glass (set $n_1 = n_0$) would reflect about 4.3%. This difference represents a significant saving of light energy in an optical system where multiple surfaces occur. For example, after only six such interfaces, or three optical components in series, 93% of the incident light survives in the case of MgF_2 coatings, compared with 77% in the case of uncoated glass.

3 TWO-LAYER ANTIREFLECTING FILMS

Durable coating materials with arbitrary refractive indices are, of course, not immediately available. Practically speaking then, single films with zero reflectances cannot be fabricated. By using a double layer of quarter-wave-thickness films, however, it is possible to achieve essentially zero reflectance at one wavelength with available coating materials. At normal incidence, the transfer

matrix of a single film of quarter-wave thickness is

$$M_1 = \begin{bmatrix} 0 & \dfrac{i}{\gamma_1} \\ i\gamma_1 & 0 \end{bmatrix}$$

The transfer matrix M for two such layers is found, according to Eq. (26), by forming the product

$$M = M_1 M_2 = \begin{bmatrix} 0 & \dfrac{i}{\gamma_1} \\ i\gamma_1 & 0 \end{bmatrix} \begin{bmatrix} 0 & \dfrac{i}{\gamma_2} \\ i\gamma_2 & 0 \end{bmatrix} = \begin{bmatrix} -\dfrac{\gamma_2}{\gamma_1} & 0 \\ 0 & -\dfrac{\gamma_1}{\gamma_2} \end{bmatrix}$$

Matrix components are $m_{11} = -\gamma_2/\gamma_1$, $m_{22} = -\gamma_1/\gamma_2$, and $m_{12} = m_{21} = 0$. Using these values in Eq. (36), the result is

$$r = \frac{\gamma_2^2\gamma_0 - \gamma_s\gamma_1^2}{\gamma_2^2\gamma_0 + \gamma_s\gamma_1^2} \tag{44}$$

Incorporating the refractive indices through the use of Eqs. (12) to (14) and then squaring to get the reflectance,

normal incidence quarter-wave thickness $$R = \left(\frac{n_0 n_2^2 - n_s n_1^2}{n_0 n_2^2 + n_s n_1^2}\right)^2 \tag{45}$$

Zero reflectance is predicted by Eq. (45) when $n_0 n_2^2 = n_s n_1^2$, or

$$\frac{n_2}{n_1} = \sqrt{\frac{n_s}{n_0}} \tag{46}$$

For a glass substrate ($n_s = 1.52$) and incidence from air ($n_0 = 1$), the ideal ratio for the two films is $n_2/n_1 = 1.23$. The requirement is met quite well using zirconium dioxide ($n_2 = 2.1$) and cerium trifluoride ($n_1 = 1.65$), both good coating materials. The ratio of refractive indices for CeF_3 and ZrO_2 of 1.27 produces a reflectance of only 0.1% according to Eq. (45). The arrangement is shown in Figure 3 and is plotted as curve (a) in Figure 4. Achieving zero reflectance at some wavelength may not satisfy the very common need to reduce reflectance over a broad region of the visible spectrum. Curve (a) is rather steep on both sides of its minimum at 550 nm. Broader regions of low reflectance result for $\lambda/4$–$\lambda/4$ coatings when the substrate index is larger than that of the adjacent film layer, that is, $n_s > n_2$. In such cases, the index is "stepped down" consistently from substrate to ambient. Indices high enough to satisfy this condition are possible in infrared applications where large values of n_s are available, as in the case of germanium with $n_s = 4$. A list of useful refractive indices is given in Table 1. Broader regions of low reflectance also become possible in the visible region of the spectrum, once the restriction of using equal $\lambda/4$ coatings is relaxed. For example, curves (b) and (c) of Figure 4 show two such solutions to the problem, where the inner coating has a thickness of $\lambda/2$, as illustrated in Figure 5. At the wavelength of 550 nm, for which the $\lambda/4$ and $\lambda/2$ thicknesses are determined, the $\lambda/2$ layer

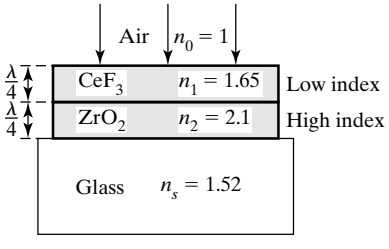

Figure 3 Antireflecting double layer, using $\lambda/4$–$\lambda/4$ thickness films.

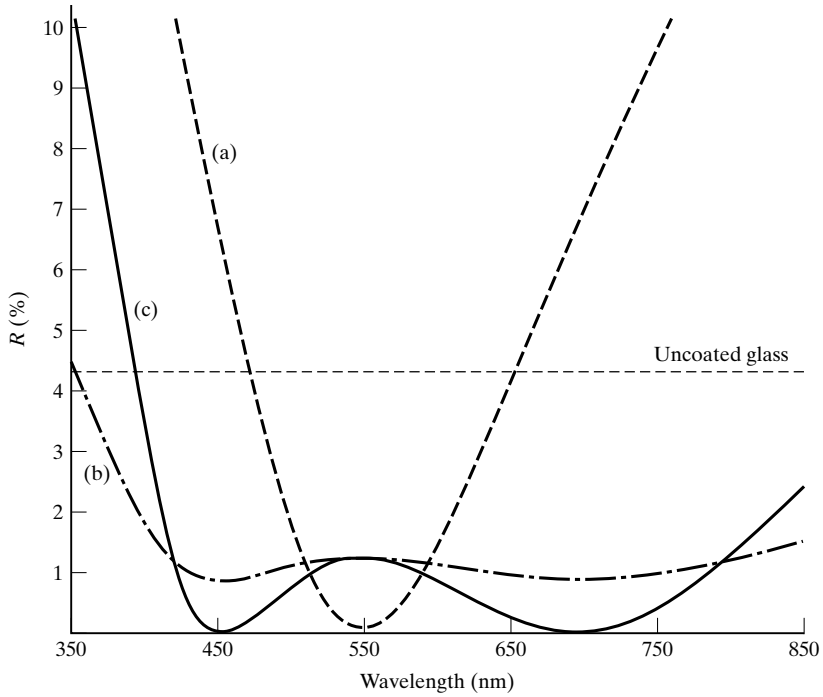

Figure 4 Reflectance from a double-layer film versus wavelength. In all cases $n_0 = 1$ and $n_s = 1.52$. Thicknesses are determined at $\lambda = 550$ nm. (a) $\lambda/4$–$\lambda/4$; $n_1 = 1.65$, $n_2 = 2.1$. (b) $\lambda/4$–$\lambda/2$: $n_1 = 1.38$, $n_2 = 1.6$. (c) $\lambda/4$–$\lambda/2$: $n_1 = 1.38$, $n_2 = 1.85$.

TABLE 1 REFRACTIVE INDICES FOR SEVERAL COATING MATERIALS

Material	Visible (~550 nm)	Near infrared (~2 μm)
Cryolite	1.30–1.33	—
MgF_2	1.38	1.35
SiO_2	1.46	1.44
SiO	1.55–2.0	1.5–1.85
Al_2O_3	1.60	1.55
CeF_3	1.65	1.59
ThO_2	1.8	1.75
Nd_2O_3	2.0	1.95
ZrO_2	2.1	2.0
CeO_2	2.35	2.2
ZnS	2.35	2.2
TiO_2	2.4	—
Si	—	3.3
Ge	—	4.0

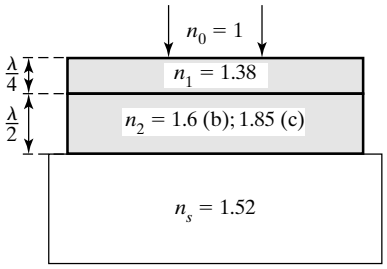

Figure 5 Antireflecting double layer using $\lambda/4$–$\lambda/2$ thickness films. Reflectance curves are shown in Figure 4.

has no effect on the reflectance and the double layer behaves like a single $\lambda/4$ layer with $R = 1.3\%$. At nearby wavelengths, however, the $\lambda/2$ layer helps to keep R below values attained by a single $\lambda/4$ layer alone. For $n = 1.85$ [curve (c)], two minima near $R = 0$ appear. Although reflectance at 550 nm is about 1.3%, greater than for the $\lambda/4$–$\lambda/4$ coating of curve (a), it remains at values less than this over the broad range of wavelengths from about 420 to 800 nm. For $n_2 = 1.6$ [curve (b)], the spectral response of the double layer, while more reflective, is flatter over the visible spectrum. Still other practical solutions for double-layer antireflecting films become possible if the thicknesses of the layers are allowed to have values other than multiples of $\lambda/4$.

The curves of Figure 4 have been calculated using the theory presented in this chapter. The overall transfer-matrix elements are first determined by forming the product of the transfer matrices of the individual layers. In these elements, the phase difference δ is expressed as a function of λ, and

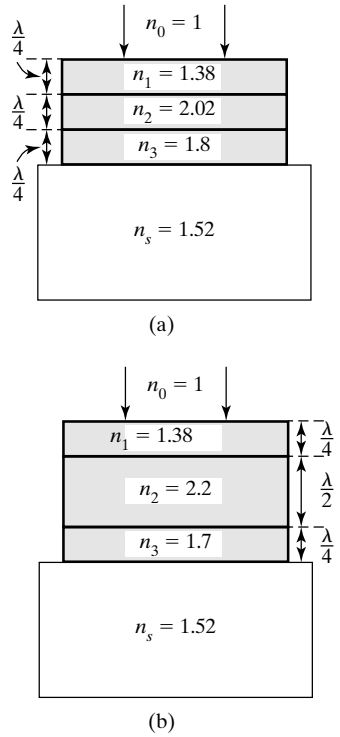

Figure 6 Antireflecting triple layers. (a) Quarter-quarter-quarter wavelength layers. (b) Quarter-half-quarter wavelength layers. Reflectance curves are shown in Figure 7.

the film thickness is determined by the $\lambda/4$ or $\lambda/2$ requirement at a single wavelength. These matrix elements are then used in Eq. (36) for the reflection coefficient. When squared, the reflectance as a function of wavelength is determined. Although the calculations can be tedious, they are easily done using a programmable calculator or computer.

4 THREE-LAYER ANTIREFLECTING FILMS

The procedure just outlined can be used to calculate the spectral reflectance of three-layer films as well. The use of three or more layer coatings makes possible a broader, low-reflectance region in which the response is flatter. If each of the three layers is of $\lambda/4$ thickness, one can show that a zero reflectance occurs when the refractive indices satisfy

$$\frac{n_1 n_3}{n_2} = \sqrt{n_0 n_s} \tag{47}$$

One such practical solution is shown in Figure 6a and plotted as curve (a) in Figure 7. Some improvement results when the middle layer is of $\lambda/2$ thickness, as in Figure 6b and curve (b) of Figure 7.

5 HIGH-REFLECTANCE LAYERS

If the order of the layers in a $\lambda/4$–$\lambda/4$ double-layer film optimized for antireflection is reversed, so that the order is air–high index–low index–substrate, all three reflected beams are in phase on emerging from the structure, and the reflectance is enhanced rather than reduced. A series of such double layers increases the reflectance further, and the structure is called a *high-reflectance stack*, or *dielectric mirror*.

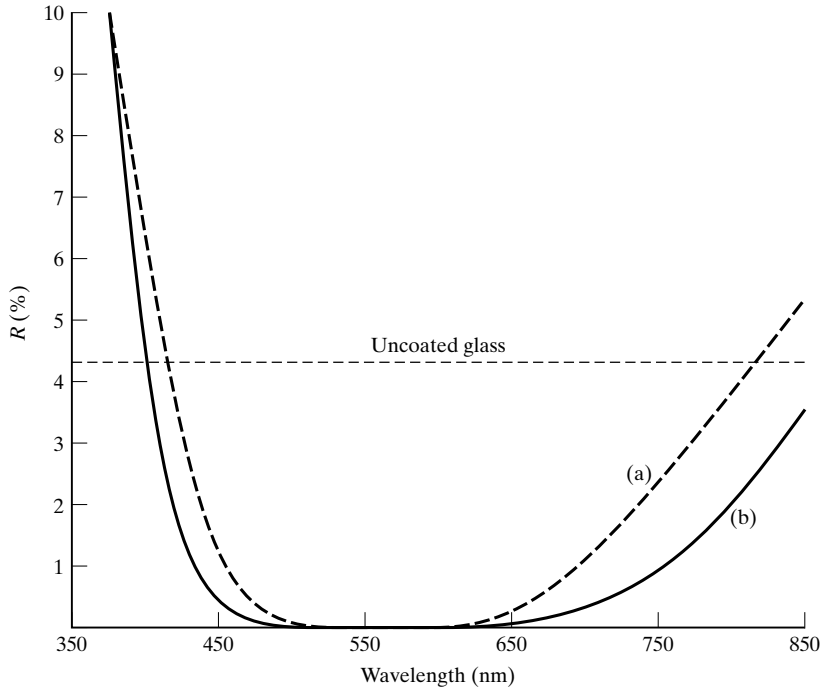

Figure 7 Reflectance from triple-layer films versus wavelength. In all cases $n_0 = 1$ and $n_s = 1.52$. Thicknesses are determined at $\lambda = 550$ nm. (a) $\lambda/4$–$\lambda/4$: $n_1 = 1.38$, $n_2 = 2.02$, $n_3 = 1.8$. (b) $\lambda/4$–$\lambda/2$–$\lambda/4$: $n_1 = 1.38$, $n_2 = 2.2$, $n_3 = 1.7$.

We derive now an expression for the reflectance of this type of structure, shown schematically in Figure 8, where High and Low signify high- and low-refractive indices, respectively. The transfer matrix for one double layer of $\lambda/4$-thick coatings at normal incidence is the product of the individual film matrices, just as in the case of the double-layer antireflecting films:

$$M_{HL} = M_H M_L$$

or

$$M_{HL} = \begin{bmatrix} 0 & \dfrac{i}{\gamma_H} \\ i\gamma_H & 0 \end{bmatrix} \begin{bmatrix} 0 & \dfrac{i}{\gamma_L} \\ i\gamma_L & 0 \end{bmatrix} = \begin{bmatrix} \dfrac{-\gamma_L}{\gamma_H} & 0 \\ 0 & \dfrac{-\gamma_H}{\gamma_L} \end{bmatrix} \tag{48}$$

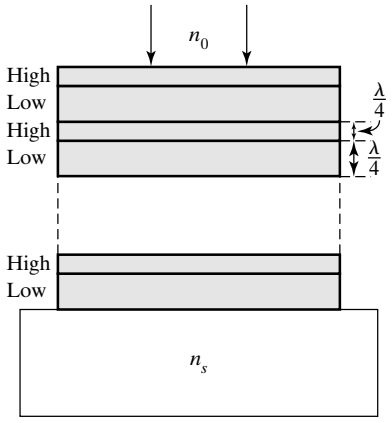

Figure 8 High-reflectance stack of double layers with alternating high- and low-refractive indices. Reflectance curves are shown in Figure 9.

For N similar double layers in series,

$$M = (M_{H1}M_{L1})(M_{H2}M_{L2}) \cdots (M_{HN}M_{LN}) = (M_H M_L)^N = (M_{HL})^N \tag{49}$$

Substituting the double-layer matrix, Eq. (48),

$$M = \begin{bmatrix} \dfrac{-\gamma_L}{\gamma_H} & 0 \\ 0 & \dfrac{-\gamma_H}{\gamma_L} \end{bmatrix}^N = \begin{bmatrix} \left(\dfrac{-\gamma_L}{\gamma_H}\right)^N & 0 \\ 0 & \left(\dfrac{-\gamma_H}{\gamma_L}\right)^N \end{bmatrix}$$

For normal incidence,

$$\frac{\gamma_L}{\gamma_H} = \frac{n_L}{n_H} \quad \text{and} \quad \frac{\gamma_H}{\gamma_L} = \frac{n_H}{n_L}$$

so that

$$M = \begin{bmatrix} \left(\dfrac{-n_L}{n_H}\right)^N & 0 \\ 0 & \left(\dfrac{-n_H}{n_L}\right)^N \end{bmatrix} \tag{50}$$

The matrix elements of the transfer matrix representing N high-low double layers of $\lambda/4$-thick coatings in series are thus

$$m_{11} = \left(\frac{-n_L}{n_H}\right)^N, \qquad m_{22} = \left(\frac{-n_H}{n_L}\right)^N, \qquad m_{12} = m_{21} = 0 \tag{51}$$

Using these matrix elements in the expression for the reflection coefficient, Eq. (36), we arrive at

$$r = \frac{n_0(-n_L/n_H)^N - n_s(-n_H/n_L)^N}{n_0(-n_L/n_H)^N + n_s(-n_H/n_L)^N} \tag{52}$$

When the numerator and denominator of Eq. (52) are next multiplied by the factor $(-n_L/n_H)^N/n_s$ and the result is squared to give reflectance, we have

$$R_{\max} = \left[\frac{(n_0/n_s)(n_L/n_H)^{2N} - 1}{(n_0/n_s)(n_L/n_H)^{2N} + 1}\right]^2 \tag{53}$$

Example 2

A high-reflectance stack like that of Figure 8 incorporates six double layers of SiO_2 ($n = 1.46$) and ZnS ($n = 2.35$) films on a glass ($n = 1.48$) substrate. What is the reflectance for light of 550 nm at normal incidence?

Solution

Substituting directly into Eq. (53), we get

$$R = \left[\frac{(1/1.48)(1.46/2.35)^{12} - 1}{(1/1.48)(1.46/2.35)^{12} + 1}\right]^2$$

or $R = 99.1\%$.

Equation (53) predicts 100% reflectance when either N approaches infinity or when (n_L/n_H) approaches zero. Some data indicating these tendencies are given in Table 2. One sees that the reflectance quickly approaches 100% for several double layers. Since the smallest ratio of n_L/n_H yields best reflectances, high-reflectance stacks may be fabricated from alternating layers of MgF_2 ($n_L = 1.38$) and ZnS ($n_H = 2.35$) or TiO_2 ($n_H = 2.40$).

The reflectance given in Eq. (53) represents the maximum reflectance at the wavelength λ_0, for which the layers have *optical* thicknesses of $\lambda_0/4$. For other wavelengths the transfer matrix must be used in its general form, containing the wavelength-dependent phase differences. Spectral reflectance curves for $N = 2$ and $N = 6$ double-layer stacks have been calculated and plotted in Figure 9. Curve (c) shows the improvement in the maximum reflectance that results for $N = 2$ stacks when an extra high-index layer is inserted between the substrate and the last low-index layer. The width of the high-reflectance region in these curves is nearly independent of the number of double layers used but increases when the ratio n_L/n_H decreases. This ratio is 0.587 in Figure 9, representing alternating MgF_2 and ZnS layers on glass. Outside the central *stopband*—the region of highest reflectance—the

TABLE 2 REFLECTANCE OF A HIGH-LOW QUARTER-WAVE STACK

Reflectance for $N = 3$ high-low layers versus n_L/n_H		Reflectance versus N when $n_L/n_H = 0.587$ for alternating double layers of MgF_2 and ZnS	
n_L/n_H	R (%)	N	R (%)
1.0	4.26	1	39.71
0.91	21.01	2	73.08
0.83	40.82	3	89.77
0.77	57.77	4	96.35
0.71	70.44	5	98.72
0.67	79.35	6	99.56
0.625	85.48	7	99.85
0.59	89.67	8	99.95
0.56	92.55		
0.53	94.56		
0.50	95.97		

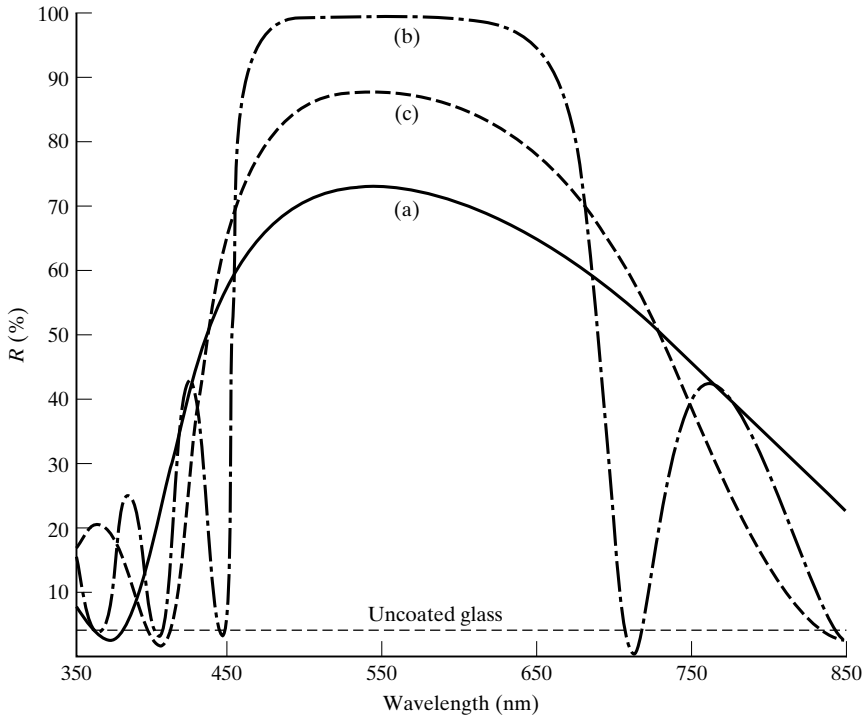

Figure 9 Spectral reflectance of a high-low index stack for (a) $N = 2$ and (b) $N = 6$ double layers. Curve (c) represents an $N = 2$ stack with an additional high-index layer adjacent to the substrate. Layers are $\lambda/4$ thick at $\lambda = 550$ nm. In all cases, $n_H = 2.35$, $n_L = 1.38$, $n_s = 1.52$, and $n_0 = 1.00$.

reflectance oscillates between a series of maxima and minima. The center of the stopband can be shifted by depositing layers whose thickness is $\lambda/4$ at another λ. Except for light energy lost by absorption and scattering during passage through the dielectric layers, the percent transmission of the structure is given by $T(\%) = 100 - R(\%)$. Thus such structures can be designed as *band-pass filters* with high spectral transmittance in the wide region of low spectral reflectance. Narrow band-pass filters that behave like Fabry-Perot etalons can be fabricated by separating two dielectric-mirror, multilayer structures with a spacer of, say, MgF_2 film. Narrow wavelength regions that satisfy constructive interference can be produced far enough apart in wavelength so that all but one such region is easily filtered out by a conventional absorption color filter. The result is a filter with a pass-band width of perhaps 15 Å and 40% transmittance.

PROBLEMS

1 Show that when the incident $\vec{\mathbf{E}}$-field is parallel to the plane of incidence, γ_1 has the form given in Eq. (37).

2 A transparent film is deposited on glass of refractive index 1.50.

a. Determine values of film thickness and (hypothetical) refractive index that will produce a nonreflecting film for normally incident light of 500 nm.

b. What reflectance does the structure have for incident light of 550 nm?

3 Show from Eq. (42) that the normal reflectance of a single half-wave thick layer deposited on a substrate is the same as the reflectance from the uncoated substrate.

$$R = \frac{(n_0 - n_s)^2}{(n_0 + n_s)^2}$$

4 A single layer of SiO_2 ($n = 1.46$) is deposited to a thickness of 137 nm on a glass substrate ($n = 1.52$). Determine the normal reflectance for light of wavelength (a) 800 nm; (b) 600 nm; (c) 400 nm. Verify the reasonableness of your results by comparison with Figure 2.

5 A 596-Å-thick layer of ZnS ($n = 2.35$) is deposited on glass ($n = 1.52$). Calculate the normal reflectance of 560 nm light.

6 Determine the theoretical refractive index and thickness of a single film layer deposited on germanium ($n = 4.0$) such that normal reflectance is zero at a wavelength of 2 μm. What actual material could be used?

7 A double layer of quarter-wave layers of Al_2O_3 ($n = 1.60$) and cryolite ($n = 1.30$) are deposited in turn on a glass substrate ($n = 1.52$).

a. Determine the thickness of the layers and the normal reflectance for light of 550 nm.
b. What is the reflectance if the layers are reversed?

8 Quarter-wave thin films of ZnS ($n = 2.2$) and MgF_2 ($n = 1.35$) are deposited in turn on a substrate of silicon ($n = 3.3$) to produce minimum reflectance at 2 μm.

a. Determine the actual thickness of the layers.
b. By what percentage difference does the ratio of the film indices differ from the ideal?
c. What is the normal reflectance produced?

9 By working with the appropriate transfer matrix, show that a quarter-wave/half-wave double layer, as in Figure 5, produces the same reflectance as the quarter-wave layer alone.

10 Write a computer program that will calculate and/or plot reflectance values for a double layer under normal incidence. Let input parameters include thickness and indices of the layers and the index of the substrate. Check results against Figure 4.

11 Prove the condition given by Eq. (47) for zero reflectance of three-layer, quarter-quarter-quarter-wave films when used with normal incidence. Do this by determining the composite transfer matrix for the three quarter layers and using the matrix elements in the calculation of the reflection coefficient in Eq. (36).

12 Using the materials given in Table 1, design a three-layer multifilm of quarter-wave thicknesses on a substrate of germanium that will give nearly zero reflectance for normal incidence of 2 μm radiation.

13 Determine the maximum reflectance in the center of the visible spectrum for a high-reflectance stack of high-low index double layers formed using $n_L = 1.38$ and $n_H = 2.6$ on a substrate of index 1.52. The layers are of equal optical thickness, corresponding to a quarter-wavelength for light of average wavelength 550 nm. The high-index material is encountered first by the incident light, as in Figure 8. Assume normal incidence and stacks of (a) 2; (b) 4; (c) 8 double layers.

14 A high-reflectance stack of alternating high-low index layers is produced to operate at 2 μm in the near infrared. A stack of four double layers is made of layers of germanium ($n = 4.0$) and MgF_2 ($n = 1.35$), each of 0.5-μm optical thickness. Assume a substrate index of 1.50 and normal incidence. What reflectance is produced at 2 μm?

15 What theoretical ratio of high-to-low refractive indices is needed to give at least 90% reflectance in a high-reflectance stack of two double layers of quarter-wave layers at normal incidence? Assume a substrate of index 1.52.

16 Show that R_{max} in Eq. (53) approaches 1 when either N approaches infinity or when the ratio n_L/n_H approaches zero.